

Dual mechanism of chromatin remodeling in the common shrew sex trivalent (XY_1Y_2)

Sergey N. Matveevsky¹, Svetlana V. Pavlova², Maret M. Atsaeva³,
Jeremy B. Searle⁴, Oxana L. Kolomiets¹

1 *N.I. Vavilov Institute of General Genetics, Russian Academy of Sciences, Gubkin str. 3, Moscow 119991, Russia* **2** *A.N. Severtsov Institute of Ecology and Evolution, Russian Academy of Sciences, Leninsky pr. 33, Moscow 119071, Russia* **3** *Chechen State University, A. Sheripov str. 32, Grozny 364051, Chechen Republic, Russia* **4** *Department of Ecology and Evolutionary Biology, Corson Hall, Cornell University, Ithaca, NY 14853, USA*

Corresponding author: Sergey N. Matveevsky (sergey8585@mail.ru)

Academic editor: A. Polyakov | Received 28 May 2017 | Accepted 26 September 2017 | Published 3 November 2017

<http://zoobank.org/D1B58C9C-D08B-4D73-9DC8-560DE40603FC>

Citation: Matveevsky SN, Pavlova SV, Atsaeva MM, Searle JB, Kolomiets OL (2017) Dual mechanism of chromatin remodeling in the common shrew sex trivalent (XY_1Y_2). *Comparative Cytogenetics* 11(4) 727–745. <https://doi.org/10.3897/CompCytogen.v11i4.13870>

Abstract

Here we focus on the XY_1Y_2 condition in male common shrew *Sorex araneus* Linnaeus, 1758, applying electron microscopy and immunocytochemistry for a comprehensive analysis of structure, synapsis and behaviour of the sex trivalent in pachytene spermatocytes. The pachytene sex trivalent consists of three distinct parts: short and long synaptic SC fragments (between the X and Y_1 and between the X and Y_2 , respectively) and a long asynaptic region of the X in-between. Chromatin inactivation was revealed in the XY_1 synaptic region, the asynaptic region of the X and a very small asynaptic part of the Y_2 . This inactive part of the sex trivalent, that we named the ‘head’, forms a typical sex body and is located at the periphery of the meiotic nucleus at mid pachytene. The second part or ‘tail’, a long region of synapsis between the X and Y_2 chromosomes, is directed from the periphery into the nucleus. Based on the distribution patterns of four proteins involved in chromatin inactivation, we propose a model of meiotic silencing in shrew sex chromosomes. Thus, we conclude that pachytene sex chromosomes are structurally and functionally two different chromatin domains with specific nuclear topology: the peripheral inactivated ‘true’ sex chromosome regions (part of the X and the Y_1) and more centrally located transcriptionally active autosomal segments (part of the X and the Y_2).

Keywords

Sex body, MSCI, synaptonemal complex, γ H2AFX, ATR, SUMO-1, ubiH2A, *Sorex araneus*

Introduction

At first meiotic prophase, the male sex chromosomes in mammals form a specific heterochromatic nuclear domain (Solari 1974; Handel 2004). The structure and behaviour of the sex bivalent changes from zygotene to late diplotene. In the majority of mammal species the processes of pairing and synapsis of the X and Y chromosomes at zygotene occurs later than the same processes in autosomes. At early and mid pachytene the sex bivalent is usually located in the centre of the meiotic nucleus. At mid pachytene the sex chromosomes become shorter due to condensation and homologous regions of the X and Y are completely paired (Burgoyne 1982). Recombination nodules appear only in the short pseudoautosomal region (PAR) of the sex bivalent. In many mammals irregular thickenings may occur at asynaptic sites of axial elements of the sex bivalent. After that the sex bivalent gradually moves from the centre of the nucleus to its periphery and forms a so-called XY or sex body (Solari 1974).

The chromatin of the sex chromosomes transforms into an inactive condition and this chromatin remodelling process is known as meiotic sex chromosome inactivation (MSCI) (McKee and Handel 1993; Turner et al. 2000). MSCI is the process whereby unsynapsed regions of the sex chromosomes undergo transcriptional silencing (Lifshytz and Lindsley 1972; Handel and Hunt 1992; Turner et al. 2002, 2007); this is a case of MSUC (meiotic silencing of unsynapsed chromatin) (Schimenti 2005). The asynaptic chromatin undergoes inactivation by incorporation and modification of specific proteins (Burgoyne et al. 2009). First, BRCA1 (breast cancer 1) accumulates in non-synaptic areas of the sex chromosomes, which starts the process of phosphokinase ATR (ataxia telangiectasia- and RAD3-related) recruitment and then there is ATR-dependent phosphorylation of the γ H2AFX (phosphorylated (Ser139) histone 2 A.X) histone (Turner et al. 2004). At early pachytene, ubiH2A (ubiquitinated histone H2A), SUMO-1 (small ubiquitin-related modifier-1) and other proteins are incorporated into the asynaptic chromatin of the sex chromosomes (Baarends et al. 2005). Such modification of chromatin decreases its transcriptional activity as confirmed using Cot-1 RNA FISH and RNA polymerase type II immunolocalisation (Turner et al. 2005; Baarends et al. 2005). Thus, the chromatin of the sex body is inactive.

MSCI has been well studied for the normal male sex chromosome system in mammals (XY), but there are few data on this process for multiple sex chromosome systems.

Translocation between the X and an autosome results in the formation of multiple sex chromosomes (XY_1Y_2 ; where the X is a product of a translocation between the 'true' X and an autosome, Y_1 is the 'true' Y and Y_2 is the autosome). The XY_1Y_2 condition has been demonstrated in insects (Jacobs 2003), fish (Centofante et al. 2006; de Oliveira et al. 2008) and, in particular, among mammals – including marsupials: greater bilby *Macrotis lagotis* (Sharp 1982), and placentals: Indian muntjac *Muntiacus muntjak* (Artiodactyla, Fronicke and Schertan 1997), red brocket deer *Mazama americana* (Artiodactyla, Aquino et al. 2013), big fruit-eating bat *Artibeus lituratus* (Chiroptera, Solari and Pigozzi 1994), short-tailed fruit bat *Carollia perspicillata* (Chiroptera, Noronha et al. 2009), delicate mouse *Salinomys delicatus* (Rodentia, Lanzone et al. 2011), Sahel gerbil *Taterillus*

arenarius and Senegal gerbil *Taterillus pygargus* (Rodentia, Ratomponirina et al. 1986; Volobouev and Granjon 1996) and others (see reviews by Fredga 1970; Sharman 1991; and Yoshida and Kitano 2012). An XY_1Y_2 sex chromosome system also characterises species of shrews (small insectivores) belonging to the *Sorex araneus* group (Eulipotyphla; Hausser et al. 1985), including the Eurasian common shrew *Sorex araneus* Linnaeus, 1758 which is a model system for evolutionary cytogenetics with numerous Robertsonian autosomal variants as well as the XY_1Y_2 condition (Searle and Wójcik 1998).

The XY_1Y_2 condition in the common shrew arises from a tandem fusion between an autosome and the true X chromosome (Sharman 1956, 1991; Fredga 1970; Searle et al. 1991) (Fig. 1a). Although the observation of a meiotic sex trivalent was part of the discovery of the XY_1Y_2 condition in the common shrew it was not until the work of Pack et al. (1993) that chromosome pairing in the XY_1Y_2 at meiotic prophase I was first examined. We supplemented those early observations with the discovery that the γ H2AFX histone is associated with the true sex chromosome regions of the pachytene sex trivalent (Matveevsky et al. 2012).

In this paper we analyse the distribution of four transcription silencing proteins (ATR, γ H2AFX, SUMO-1, ubiH2A) on the sex trivalent XY_1Y_2 at prophase I in common shrew spermatocytes and assess how these participate in MSCI.

Material and methods

Shrews. A total of five adult males of the common shrew were collected from a locality in the vicinity of the Moscow-Neroosa chromosomal hybrid zone (near Ozyory town, Moscow Region) in April 2014, at the beginning of the breeding season. All animals were karyotyped using the method of Pavlova et al. (2008), with modifications. The trypsin-Giemsa staining technique of Král and Radjabli (1974) was used for identification of chromosome arms by G-bands, following the standard nomenclature for the *S. araneus* karyotype, which uses letters of the alphabet for chromosome arms (Searle et al. 1991).

All karyotypes were characterised by the set of invariant autosomal metacentrics *af*, *bc*, *jl* and *tu* as well as the XY_1Y_2 sex chromosomes system. Race-specific autosomes differed between individuals, two males had *gm*, *hi*, *kr*, *no* and *pq* metacentrics which mark the karyotype of the Moscow race. Other males had *go*, *hi*, *kr*, *mn* and *pq* metacentrics which characterise the Neroosa race. All shrews had the same diploid number of chromosomes ($2n=21$). Spermatocyte spreads were obtained from all males. All necessary national and institutional guidelines for the care and use of animals were followed.

A total of 331 cells were analysed of which 14 were prepared for electron microscopy and 317 for fluorescence microscopy. All the latter were labelled with SYCP3 (synaptonemal complex protein 3) and CREST and a proportion of cells were labelled with other antibodies (γ H2AFX: 90; SUMO-1: 59; ubiH2A: 52; ATR: 32; MLH1: 74; SYCP1: 28; RNA Pol II: 10).

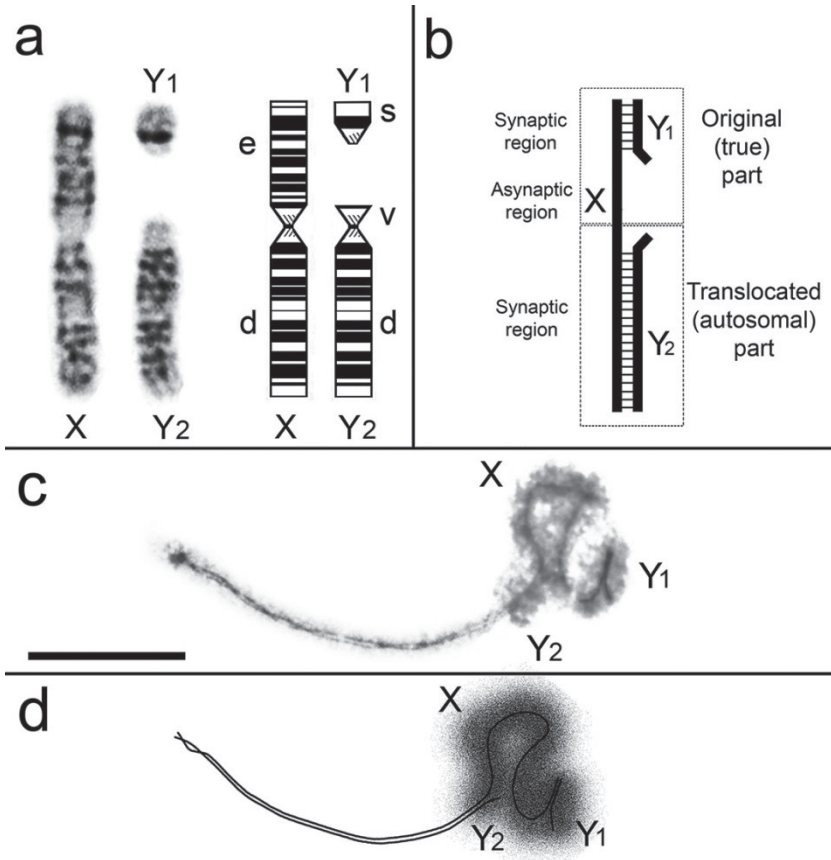


Figure 1. **a** G-banded sex chromosomes in the male common shrew (left) and ideogram with chromosome arms labelled according to the alphabetic nomenclature of Searle et al. (1991) **b** Schematic diagram of the shrew pachytene sex trivalent, based on Pack et al. (1993) and our data **c** Electron micrograph of a shrew sex trivalent, XY_1Y_2 at late pachytene. The true X region and the Y_1 are surrounded by electron-dense material. Scale bar: $5\mu\text{m}$. **d** Diagram of the XY_1Y_2 configuration as represented in Fig. 1c.

Meiotic spread preparations. Synaptonemal complex (SC) preparations were made and fixed using a previously described technique (Kolomiets et al. 2010). AgNO_3 -stained slides were screened under a light microscope to select suitably spread cells. Once selected, plastic (Falcon film) circles were cut out with a diamond tip and transferred onto grids and examined in a JEM 100B electron microscope.

Antibodies, immunocytochemistry and multistep immunostaining procedure. Poly-L-lysine-coated slides were used for immunostaining. The slides were placed in phosphate buffer saline (PBS) and incubated overnight at 4°C with the primary antibodies diluted in antibody dilution buffer (3% bovine serum albumin - BSA, 0.05% Triton X-100 in PBS): mouse anti-MLH1 (1:50–1:100, Abcam, Cambridge, UK), rabbit polyclonal anti-SYCP1 (1:500, Abcam, Cambridge, UK), rabbit polyclonal anti-SYCP3

(1:500–1:1000, Abcam, Cambridge, UK), mouse monoclonal anti-ATR (1:200, Abcam, Cambridge, UK), human anticentromere antibody CREST (Calcinosis Raynaud's phenomenon, Esophageal dysmotility, Sclerodactyly, and Telangiectasia) (1:500, Fitzgerald Industries International, Acton, MA, USA), mouse monoclonal anti-SUMO-1 (1:250, Zymed Laboratories, South San Francisco, CA, USA), mouse monoclonal anti-ubiquityl histone H2A (1:400, Millipore, Billerica, MA, USA), and mouse anti-phospho-histone H2AX (also known as γ H2AFX) (1:1000, Abcam, Cambridge, UK).

After washing, we used the following corresponding secondary antibodies diluted in PBS: FITC-conjugated bovine anti-rabbit IgG (1:1000, Santa Cruz Biotechnology, Santa Cruz, CA, USA), goat anti-rabbit Alexa Fluor 488 (1:500, Invitrogen Corporation, Carlsbad, CA, USA), FITC-conjugated horse anti-mouse IgG (1:500, Vector Laboratories, Burlingame, CA, USA), Rodamin-conjugated chicken anti-rabbit IgG (1:400, Santa Cruz Biotechnology, Santa Cruz, CA, USA), goat anti-human Alexa Fluor 546 (1:500, Invitrogen Corporation, Carlsbad, CA, USA), goat anti-mouse Alexa Fluor 546 (1:200, 1:1000, Invitrogen Corporation, Carlsbad, CA, USA).

Immunostaining was carried out sequentially in 3 steps: 1. SYCP3/CREST (or SYCP1/MLH1); 2. ATR (or SUMO-1 or ubiH2A); 3. γ H2AFX. After an each step slides were washed in PBS (6–7 times for 7–10 min) and mounted with Vectashield mounting medium containing 4,6-diamino-2-phenylIndol (DAPI) (Vector Laboratories, Burlingame, CA, USA). Slides were examined using an Axioimager D1 microscope (Carl Zeiss, Jena, Germany) equipped with an AxioCam HRm CCD camera. Images were processed using Adobe Photoshop CS3 Extended.

It should be noted that after photobleaching, bound antibodies of the first round still remain attached to the cellular structures. The more antibodies attached to the structures of interest the higher the probability that epitopes of further rounds of immunolocalisation become inaccessible. To ensure that these processes have not impacted our results, we performed control experiments for all antibodies.

Controls. We always conducted parallel control experiments on different slides when immunostaining was performed with a single antibody to a MSCI specific protein (double immunostaining). Our colleague Dr TM Grishaeva has conducted a bioinformatics analysis of the proteins studied. The pairwise sequence alignment of human and mouse proteins, which was performed by the COBALT program (NCBI), demonstrated high conservation of the H2AX, ubiH2A, SUMO-1, ATR and Polo II proteins. Comparison of the proteins did not reveal any problematic similarity between them. The pairwise sequence alignment of ATR and H2AX showed no amino acid sequence similarity. SUMO-1 and H2AX appeared to have 14 coincidences of amino acids, which should not affect the cross-reaction. ubiH2A and H2AX have a high level of similarity except a short sequence in the carboxyl terminus. Nevertheless, an analysis of the fluorescence intensity profile suggests a close, but not identical, picture of distribution for ubiH2A and H2AX (Matveevsky et al. 2016).

Image analysis. Intensity Correlation Analysis (ICA) was carried out according to Reitan et al. (2012). Scatter plots, Pearson's coefficients (ρ_r) and overlap correlation coefficients (r) were obtained using a plug-in ICA (Li et al. 2004) of ImageJ 1.45 (Ras-

band 1997–2016). p_r helps to evaluate the degree of correlation between the different intensities and is ranked from -1 (negative correlation) to +1 (positive correlation) (French et al. 2008). In analysing scatter plots, overlaying green and red signal resulted in a yellow signal. The more yellow in the scatter plot, the higher the level of overlap. The width of the yellow signal distribution in scatter plots corresponded to the degree of co-localisation of the fluorescence signals being compared: the wider the distribution of the signal, the higher the level of overlap of the two channels.

To evaluate the degree of co-localisation of some proteins, we have developed Fluorescent-Intensity Profiles (FIPs) using the ImageJ plug-in RGB profiler (created by Christophe Laummonerie, Jerome Mutterer, Institute de Biologie Moleculaire des Plantes, Strasbourg, France) and following Barak et al. (2010) and Fargue et al. (2013).

Statistical analysis. All of the data are shown as the mean values \pm SD. Student's *t*-test was performed to determine significant differences in the data. All statistical analyses were conducted using GraphPad Prism Version 5.0 (GraphPad Software, CA, USA).

Results

Synapsis and markers of recombination of the XY_1Y_2 configuration at pachytene

The sex trivalent XY_1Y_2 was detected in spermatocyte nuclei from the beginning of the early pachytene stage in electron micrographs. Three distinct parts are clearly visible on the sex trivalent: short and long synaptic SC segments and a long asynaptic segment of the X chromosome arranged between them. The first (short) segment of the SC (the PAR synaptic site) is formed between the true X region and the Y_1 and is always located at the periphery of a nucleus. The second (long) segment is the SC between the translocated (autosomal) part of the X chromosome and the Y_2 (Fig. 1); this fragment is always directed into the spermatocyte nucleus. The axial element of the X chromosome is irregularly thickened in the asynaptic region that sits between the two synaptic regions.

At the early stages of prophase I, the length of the SC between the autosomal part of the trivalent (X and Y_2) is variable. At late zygotene and early pachytene, synapsis was observed along the entire length of the segment; while in mid pachytene desynapsis of chromosome arm *v* of Y_2 (Fig. 1a) was detected. The length of this desynaptic segment was about 3–4% of the total length of Y_2 (Fig. 1b).

At mid-late pachytene, a cloud of electron-dense material overlays the true sex chromosome regions which include the region of XY_1 synapsis, the asynaptic part of the X chromosome, a short pericentromeric segment of the SC between the X and Y_2 and the asynaptic part of the Y_2 (Fig. 1c–d). Thus, it is precisely this part of the XY_1Y_2 that takes the form of the typical sex body in male mammals.

Immunostaining with antibodies against the proteins of the axial (SYCP3) and central (SYCP1) elements of the SC revealed the differences in the distribution pat-

terns of these proteins in the sex trivalent structure. SYCP3 and SYCP1 foci were always displayed evenly and clearly on the long synaptic SC (between the Y₂ and translocated part of the X), while the distribution foci of these proteins were either fragmentary (Fig. 2a, f, k) or completely absent in the case of SYCP1 (Fig. 2p, p', p'') on the short PAR synaptic fragment of SC (between the Y₁ and the true X region).

Centromeres of the sex trivalent were detected using CREST serum. One centromere was located on the Y₁ acrocentric and a second was seen where the X and the Y₂ associated. Sometimes two centromeric signals were detected in this long synaptic fragment of the SC. Thus, localisation of the X and Y₂ centromeres in the structure of the sex trivalent does not coincide.

Late recombination nodules were detected using antibodies to MLH1 (MutL homolog 1; a DNA mismatch repair protein component that is specific to these nodules). In the structure of the sex trivalent one MLH1 focus is located on the short PAR synaptic site (where the Y₁ and the true part of X pair) and another one where the Y₂ and translocated part of X pair (Fig. 2q).

MSCI markers distribution in the pachytene XY₁Y₂

The distribution of the four transcriptional silencing proteins was analysed using immunostaining. ATR had a discontinuous localisation in the true sex chromosome regions, including a few ATR foci in the region of XY₁ synapsis (Fig. 2a–e).

As a rule, as shown in our previous work on common shrews (Matveevsky et al. 2012), γ H2AFX is also associated with the true sex chromosome regions within the XY₁Y₂, including chromatin of the asynaptic region of the X chromosome. It should be noted that the histone γ H2AFX extends into the autosomal centromeric region of the XY₁Y₂ (Figs 2c, h, m, 3).

SUMO-1 is also localised only in the true sex chromosome regions, adjacent to the axial elements of the sex trivalent. Unlike the continuous distribution of γ H2AFX, SUMO-1 has a granular pattern of localisation. The chromatin of the translocated part of XY₁Y₂ does not become immunostained with antibodies to the SUMO-1 (Figs 2f–j, 3).

Localisation of ubiH2A looks like an extensive cloud around the true X chromosome and Y₁ only without extending to the autosomal part of the XY₁Y₂ (Figs 2k–o, 3).

ICA and FIPs allowed us to estimate the degree of MSCI protein co-localisation (Fig. 2c', h', m'). This was high for γ H2AFX and ubiH2A ($r_p = 0.86 \pm 0.06$, $r = 0.92 \pm 0.04$; n=22) (see Fig. 4). Regarding the FIPs, the γ H2AFX-signal path was similar to the ubiH2A-signal path, but slightly wider in coverage (Fig. 2m'). The degree of γ H2AFX / SUMO-1 co-localisation was lower ($r_p = 0.76 \pm 0.09$, $r = 0.86 \pm 0.07$; n=30) (see Fig. 4). The SUMO-1 signal occupies a narrower part of the X axis and shows three peaks within the chromatin around the XY₁ pairing region (Fig. 2h'). A significant low degree of co-localisation was found for the γ H2AFX / ATR pair ($r_p = 0.38 \pm 0.08$, $r = 0.58 \pm 0.09$; n=10), as evident in Fig. 2c (see Fig. 4). The ATR-signal path has two peaks

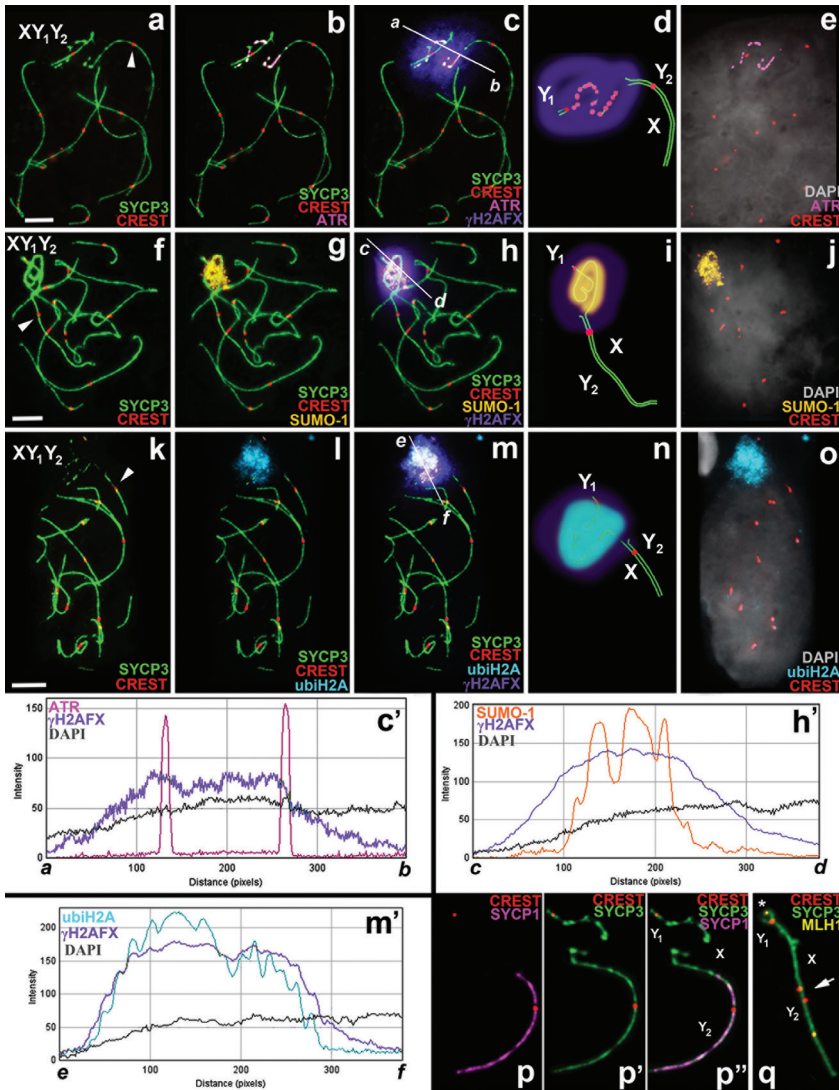


Figure 2. Mid-pachytene spermatocytes and male sex (XY_1Y_2) chromosomes of *Sorex araneus*. Bar = $5\mu\text{m}$. The axial elements of the SC and the kinetochores were localised using anti-SYCP3 (green) and anti-CREST (red) antibodies, respectively. **a–e** ATR (magenta) has a discontinuous localisation within the chromatin of the true sex chromosome regions (part of the X and the Y_1). The co-localisation of ATR, γH2AFX (violet), DAPI (grey) is shown in graph *a–b* (see **c** and **c'**) **f–j** SUMO-1 (yellow) is localised on the chromatin of true sex chromosome regions. The co-localisation of SUMO-1, γH2AFX (violet) and DAPI (grey) is shown in graph *c–d* (see **h** and **h'**) **k–o** ubiH2A (cyan) is localised on the chromatin of the true sex chromosome regions. The co-localisation of ubiH2A, γH2AFX (violet) and DAPI (grey) is shown in graph *e–f* (see **m** and **m'**) **d, i, n** Diagrams of the sex trivalents **p, p', p''** SYCP1 (magenta) is located on the area of chromosome synapsis of the autosomal part of the XY_1Y_2 (from **a–c**) **q** XY_1Y_2 has two MLH1 signals (yellow). The MLH1 signal within the PAR synaptic site is marked by an asterisk. The arrowhead indicates the centromeres of the autosomal part of sex trivalent (part of the X and the Y_2) which are not co-oriented with each other (red).

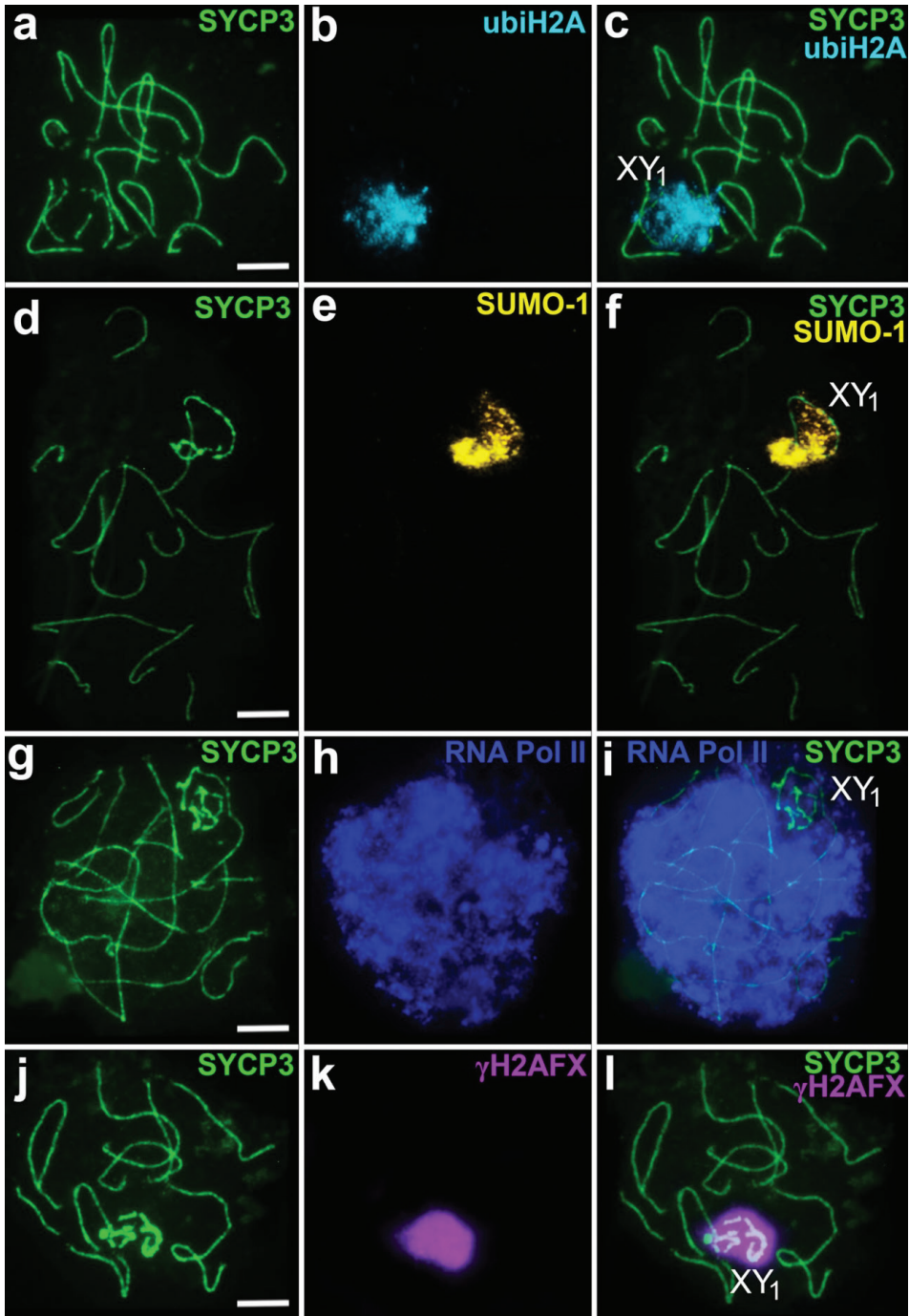


Figure 3. Mid-pachytene spermatocytes of *Sorex araneus*. Double immunostaining with antibodies: **a–c** anti-SYCP3 (green)/anti-ubiH2A (cyan) **d–f** anti-SYCP3 (green)/anti-SUMO-1 (yellow) **g–i** anti-SYCP3 (green)/anti-RNA Pol II (blue) **j–l** anti-SYCP3 (green)/anti- γ H2AFX (violet). The true sex chromosome region is designated as XY_1 . Scale bars: 5 μ m.

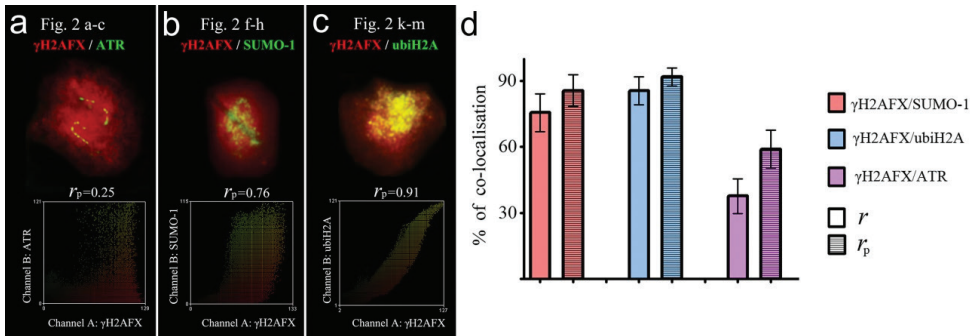


Figure 4. Intensity correlation analysis (ICA) represented by scatter plots showing the paired intensities of two channels (**a** γ H2AFX - ATR, Fig. 2a–c **b** γ H2AFX - SUMO-1, Fig. 2f–h **c** γ H2AFX - ubiH2A Fig. 2k–m). r_p - Pearson correlation coefficient. See more details in the text. Degree of co-localisation for signals in sex trivalents of common shrew (**d**). On the y -axis, the percentage of co-localised signals are shown according to overlap correlation coefficients (r) and the Pearson correlation coefficient (r_p).

in the sites of the crossing ATR- and SYCP3-signals and is not synchronised with the γ H2AFX-signal path (Fig. 2m').

The RNA Pol II intensively immunostained the whole nucleus, except for the zone where the true part of the sex trivalent is located. In this area the signal is reduced (Fig. 3g–i).

Discussion

Specific features of synaptic and recombination behaviour of the XY_1Y_2 at pachytene

The sex chromosomes (XY_1Y_2) in the common shrew were originally described by Sharman (1956). Later studies of total preparations of SC by light microscopy did not reveal details of XY_1Y_2 synapsis at prophase I (Wallace and Searle 1990; Mercer et al. 1992); these were described using electron microscopy (Pack et al. 1993; Narain and Fredga 1997). It was found that the sex trivalent forms an argyrophilic sex body that moves to the nucleus periphery during prophase I. It is interesting that the autosomal part of the sex trivalent is directed into the meiotic nucleus. A similar synapsis of sex chromosomes and the formation of electron-dense material around the true sex chromosome regions within the XY_1Y_2 trivalent were identified previously in the bat *Artibeus lituratus* (Solari and Pigozzi 1994) and the deer *Mazama americana* (Aquino et al. 2013). A similar pattern of synapsis in the sex trivalent was also detected in some species of gerbils (Wahrman et al. 1983; Ratomponirina et al. 1986) and in the muntjac; however, in the last case it was difficult to identify clearly the synaptic participants in the absence of electron micrographs (Pathak and Lin 1981).

Desynapsis of the short peritelomeric segment of Y_2 within the sex trivalent (i.e. chromosome arm v : Fig. 1a) has previously been described for several species including the aforementioned bats, deer and gerbils and Pack et al. (1993) already mentioned

this phenomenon for the common shrew. From G-banding it looks as if the chromosome arm ν on the Y₂ is homologous to an equivalent region on the X chromosome (Fig. 1a). Thus, the desynapsis may be an unusual behaviour of homologous chromatin in proximity to the chromosomal breakpoint of the X-autosome tandem fusion. However, further studies are needed to establish whether the chromosome arm ν on the Y₂ is truly homologous to the equivalent region on the X chromosome.

Our data show that each part of the XY₁Y₂, the true sex chromosome regions and the translocated parts, displayed one signal of a recombination nodule. A similar pattern of recombination events was revealed previously in common shrew spermatocytes (Borodin et al. 2008) but sometimes these authors visualised two MLH1 signals on the autosomal part of the trivalent, although there usually was a single signal. So, in general features, our results confirmed previous data.

Chromatin remodelling in the pachytene XY₁Y₂

The study of chromatin remodelling of the sex body is possible by immunodetection of specific epigenetic MSCI markers, such as BRCA1, ATR, γ H2AFX, SUMO-1 and ubiH2A (Mahadevaiah et al. 2008; Manterola et al. 2009; Page et al. 2012; Sciarano et al. 2012, 2013; Matveevsky et al. 2016; and others). It has previously been found that ATR, γ H2AFX, SUMO-1 and ubiH2A play some role in maintaining an inactive form of the chromatin and, in general, in the formation of the sex body (Moens et al. 1999; Mahadevaiah et al. 2001; Rogers et al. 2004; Cao and Yan 2012). In shrew spermatocytes, MSCI starts with the appearance of ATR in the asynaptic region of the X chromosome. After that, the second wave of γ H2AFX phosphorylation covers the chromatin associated with the true sex chromosome regions, as shown in our previous work (Matveevsky et al. 2012). Both SUMO-1 and ubiH2A appear simultaneously on the sex trivalent. This picture of MSCI is typical for the XY chromosomes of most mammals, including rodents (Turner 2007; Namekawa and Lee 2009). But the chromatin of the shrew sex trivalent has some distinguishing features, for example, ATR and SUMO-1 are narrowly localised along the axial/lateral elements in both the XY₁ synaptic region and the asynaptic region within the sex trivalent. We have not seen the spread of the ATR signal into the surrounding chromatin. In contrast, in mice ATR is immunostained along the asynaptic elements with a less intense signal extending into the surrounding chromatin (Turner et al. 2004; Manterola et al. 2009; Fedoriw et al. 2015) and in the mole vole an intense ATR signal surrounds the entire sex bivalent (Matveevsky et al. 2016). SUMO-1 covers the asynaptic region as an extensive cloud in mice (La Salle et al. 2008; Manterola et al. 2009). At the same time, γ H2AFX and ubiH2A are as widely distributed over the shrew sex chromatin as in mice and other species (de la Fuente et al. 2007; Sciarano et al. 2012, 2013). Although the chromatin organisation in mammals is universal, a special feature of the epigenetic landscape of sex chromatin has been shown in horses (Baumann et al. 2011) and in human (Metzler-Guillemain et al. 2008). In this case γ H2AFX does not cover the chromatin

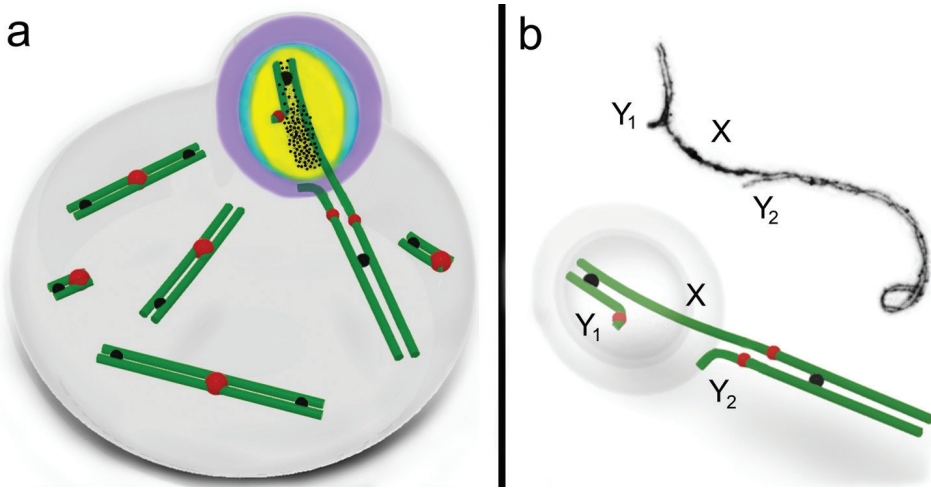


Figure 5. Schematic illustration of male common shrew MSCI. A mid-pachytene spermatocyte (**a**) and a sex (XY_1Y_2) trivalent (**b**) of a shrew are shown. An electron micrograph of the sex trivalent is shown at the top of the **b**. The true sex chromosome regions (part of the X and the Y_1) form a sex body on the periphery of the nucleus. The chromatin of the sex body undergoes reorganisation. MSCI markers have different distributions: SUMO-1 (yellow), ATR (black dots), ubiH2A (blue), γ H2AFX (violet). ATR is localised on the true sex chromosome regions, and is especially intense on the asynaptic region with a smaller amount where there is synapsis. SUMO-1 and ubiH2A are localised on both the asynaptic and synaptic regions of the true sex chromosome regions. γ H2AFX overlays all the true sex chromosome regions and the unpaired part of the Y_2 axial element. Representative autosomal SCs are shown. MLH1 signals are shown as black balls. The red balls indicate centromeres.

but is localised to the axial elements of the sex bivalent, while ubiH2A is completely absent from the sex body. It is obvious that different epigenetic markers of MSCI may be species-specific features. It is worth noting that we analysed the distribution of the mouse monoclonal ubiH2A, E6C5 clone, while the rabbit monoclonal ubiH2A, D27C4 clone, generates different results (Hasegawa et al. 2015).

The proteins around the true sex chromosome regions of the XY_1Y_2 are argentophilic and so the electron-dense cloud is detected around the site of synapsis between X and Y_1 , the unpaired region of the X chromosome, the desynaptic part of the Y_2 and a short pericentromeric synaptic site between X and Y_2 (Fig. 1a–d).

On the basis of immunocytochemistry of MSCI proteins, in this study we suggest a chromatin remodelling model in shrew pachytene spermatocytes (Fig. 5), including two different structural and functional chromatin domains within the sex trivalent: the inactivated chromatin of the true sex chromosome regions and the absence of inactivation in the translocated part. The true sex chromosome regions within the sex trivalent form a macrochromatin domain with both universal and specific features of MSCI, while the translocated part is a typical autosomal chromatin domain. Our interpretations are strongly supported by the distributions of proteins as observed in the preparations, with substantial replication and care in immunostaining and no indications

of artefacts that are always a possibility with the spreading technique and efficiency of antibody affinity/sensitivity.

It is worth noting that Pack et al. (1993) assumed, without firm evidence, that the translocated component of the XY₁Y₂ in common shrews does not likely undergo inactivation; similar assumptions have been made for other species such as the sex trivalent in the big fruit-eating bat (Solari and Pigozzi 1994). We have been able to use immunological markers to demonstrate that the autosomal component of the sex trivalent (excluding the unpaired part of Y₂) in the common shrew remains free of the chromatin modifications associated with MSCI.

Thus, our study shows that the shrew sex trivalent (XY₁Y₂) has a similar scenario of synapsis and meiotic silencing of unsynapsed chromatin (MSCI) processes as found in the usual sex chromosomes (XY) of male mammals. Apparently, this particular X-autosome translocation does not change the behaviour of the true sex chromosome regions in meiosis and does not affect the process of chromatin transformation at prophase I.

Thus, we may conclude that remodelling of sex chromatin in shrew spermatocytes neatly fits into the MSCI concept.

Conclusion

A pronounced difference in the structure, behaviour and MSCI of the two parts of the shrew sex trivalent has been revealed on the basis of detailed analysis of the organisation and behaviour of XY₁Y₂ at prophase I of meiosis. The 'head' part of the trivalent that moves to the periphery of the pachytene nuclei involves the true sex chromosome regions and includes synapsis between the X and Y₁ chromosomes. The 'tail' part involves the region of synapsis between the translocated X and Y₂ chromosomes. The structure and behaviour of the 'head' part (true X region and the Y₁) including specific MSCI shows patterns which are typical for a male sex bivalent of mammals. At the same time, the 'tail' part (the translocated region of the X and the Y₂) is located among other autosomes and does not differ from them morphologically excluding the fact that this part is attached to the 'head' part of the sex trivalent. These dual properties of the 'head' and 'tail' parts of the XY₁Y₂ trivalent in shrew spermatocytes are a notable feature of this system.

It is also noteworthy in this study that we have determined for the first time specific features of MSCI related to the discontinuous distribution of ATR along the SC at the site of synapsis between X and Y₁ and the distribution limits of SUMO-1 which occurs in the same part of the SC.

Acknowledgements

We are grateful to G.N. Davidovich and A.G. Bogdanov of the Electron Microscopy Laboratory of Biological Faculty of Moscow State University for the technical assis-

tance and to the reviewers for their helpful comments. We thank the Common Use Center of the Vavilov Institute of General Genetics of the Russian Academy of Sciences for the possibility to use some microscopic equipment. This work was partially supported by research grants of the Russian Foundation for Basic Research № 15-29-02649 (to SM), 16-04-01447 (to OL), 15-04-04759 (to SP) and the President Grant for Russian Distinguished Young Scientists MK-4496.2015.4 (to SP).

References

- Aquino CI, Abril VV, Duarte JMB (2013) Meiotic pairing of B chromosomes, multiple sexual system, and Robertsonian fusion in the red brocket deer *Mazama americana* (Mammalia, Cervidae). *Genetics and Molecular Research* 12: 3566–3574. <https://doi.org/10.4238/2013.September.13.1>
- Baarends WM, Wassenaar E, van der Laan R, Hoogerbrugge J, Sleddens-Linkels E, Hoeijmakers JH, de Boer P, Grootegoed JA (2005) Silencing of unpaired chromatin and histone H2A ubiquitination in mammalian meiosis. *Molecular and Cellular Biology* 25: 1041–1053. <https://doi.org/10.1128/MCB.25.3.1041-1053.2005>
- Barak B, Williams A, Bielopolski N, Gottfried I, Okun E, Brown MA, Matti U, Rettig J, Stuenkel EL, Ashery U (2010) Tomosyn expression pattern in the mouse hippocampus suggests both presynaptic and postsynaptic functions. *Frontiers in Neuroanatomy* 4: 1–11. <https://doi.org/10.3389/fnana.2010.00149>
- Baumann C, Daly CM, McDonnell SM, Viveiros SM, de la Fuente R (2011) Chromatin configuration and epigenetic landscape at the sex chromosome bivalent during equine spermatogenesis. *Chromosoma* 120: 227–244. <https://doi.org/10.1007/s00412-010-0306-5>
- Borodin PM, Karamysheva TV, Belonogova NM, Torgasheva AA, Rubtsov NB, Searle JB (2008) Recombination map of the common shrew, *Sorex araneus* (Eulipotyphla, Mammalia). *Genetics* 178: 621–632. <https://doi.org/10.1534/genetics.107.079665>
- Bulatova N, Searle JB, Bystrakova N, Nadjafova R, Shchipanov N, Orlov V (2000) The diversity of chromosome races in *Sorex araneus* from European Russia. *Acta Theriologica* 45: 33–46. <https://doi.org/10.4098/AT.arch.00-60>
- Burgoyne PS (1982) Genetic homology and crossing over in the X and Y chromosomes of mammals. *Human Genetics* 61: 85–90. <https://doi.org/10.1007/BF00274192>
- Burgoyne PS, Mahadevaiah SK, Turner JM (2009) The consequences of asynapsis for mammalian meiosis. *Nature Reviews Genetics* 10: 207–216. <https://doi.org/10.1038/nrg2505>
- Cao J, Yan Q (2012) Histone ubiquitination and deubiquitination in transcription, DNA damage response, and cancer. *Frontiers in Oncology* 2: 1–9. <https://doi.org/10.3389/fonc.2012.00026>
- Centofante L, Bertollo LAC, Moreira-Filho O (2006) Cytogenetic characterization and description of an XX₁XY₁Y₂ sex chromosome system in catfish *Harttia carvalhoi* (Siluriformes, Loricariidae). *Cytogenetic and Genome Research* 112: 320–324. <https://doi.org/10.1159/000089887>

- de la Fuente R, Parra MT, Viera A, Calvente A, Gomez R, Suja JA, Rufas JS, Page J (2007) Meiotic pairing and segregation of achiasmatic sex chromosomes in eutherian mammals: the role of SYCP3 protein. *PLoS Genetics* 3: e198. <https://doi.org/10.1371/journal.pgen.0030198>
- de la Fuente R, Manterola M, Viera A, Parra MT, Alsheimer M, Rufas JS, Page J (2014) Chromatin organization and remodeling of interstitial telomeric sites during meiosis in the Mongolian gerbil (*Meriones unguiculatus*). *Genetics* 197: 1137–1151. <https://doi.org/10.1534/genetics.114.166421>
- de Oliveira RR, Feldberg E, Anjos MB, Zuanon J (2008) Occurrence of multiple sexual chromosomes (XX/XY₁Y₂ and Z₁Z₁Z₂Z₂/Z₁Z₂W₁W₂) in catfishes of the genus *Ancistrus* (Siluriformes, Loricariidae) from the Amazon Basin. *Genetica* 134: 243–249. <https://doi.org/10.1007/s10709-007-9231-9>
- de Vries FA, de Boer E, van den Bosch M, Baarends WM, Ooms M, Yuan L, Liu JG, van Zee-land AA, Heyting C, Pastink A (2005) Mouse Sycp1 functions in synaptonemal complex assembly, meiotic recombination, and XY body formation. *Genes & Development* 19: 1376–1389. <https://doi.org/10.1101/gad.329705>
- Fargue S, Lewin J, Rumsby G, Danpure CJ (2013) Four of the most common mutations in primary hyperoxaluria type 1 unmask the cryptic mitochondrial targeting sequence of alanine:glyoxylate aminotransferase encoded by the polymorphic minor allele. *Journal of Biological Chemistry* 288: 2475–2484. <https://doi.org/10.1074/jbc.M112.432617>
- Fedoriw AM, Menon D, Kim Y, Mu W, Magnuson T (2015) Key mediators of somatic ATR signaling localize to unpaired chromosomes in spermatocytes. *Development* 142: 2972–2980. <https://doi.org/10.1242/dev.126078>
- Fernandez-Capetillo O, Mahadevaiah SK, Celeste A, Romanienko PJ, Camerini-Otero RD, Bonner WM, Manova K, Burgoyne P, Nussenzweig A (2003) H2AX is required for chromatin remodeling and inactivation of sex chromosomes in male mouse meiosis. *Developmental Cell* 4: 497–508. [https://doi.org/10.1016/S1534-5807\(03\)00093-5](https://doi.org/10.1016/S1534-5807(03)00093-5)
- Fredga K (1970) Unusual sex chromosome inheritance in mammals. *Philosophical Transactions of the Royal Society of London B* 259: 15–36. <https://doi.org/10.1098/rstb.1970.0042>
- French AP, Mills S, Swarup R, Bennett MJ, Pridmore TP (2008) Colocalization of fluorescent markers in confocal microscope images of plant cells. *Nature Protocols* 3: 619–628. <https://doi.org/10.1038/nprot.2008.31>
- Fronicke L, Scherthan H (1997) Zoo-fluorescence in situ hybridization analysis of human and Indian muntjac karyotypes (*Muntiacus muntjak vaginalis*) reveals satellite DNA clusters at the margins of conserved syntenic segments. *Chromosome Research* 5: 254–261. <https://doi.org/10.1023/B:CHRO.0000032298.22346.46>
- Handel MA, Hunt PA (1992) Sex-chromosome pairing and activity during mammalian meiosis. *Bioessays* 14: 817–822. <https://doi.org/10.1002/bies.950141205>
- Handel MA (2004) The XY body: a specialized meiotic chromatin domain. *Experimental Cell Research* 296: 57–63. <https://doi.org/10.1016/j.yexcr.2004.03.008>
- Hausser J, Catzeflis F, Meylan A, Vogel P (1985) Speciation in the *Sorex araneus* complex (Mammalia, Insectivora). *Acta Zoologica Fennica* 170: 125–130.

- Jacobs DH (2003) Cytogenetics of the genus *Dundocoris* Hoberlandt (Heteroptera, Aradidae, Carventinae) where chromosome fusion played the dominant role in karyotype evolution. *Caryologia* 56: 233–252. <https://doi.org/10.1080/00087114.2003.10589331>
- Kolomiets OL, Matveevsky SN, Bakloushinskaya IY (2010) Sexual dimorphism in prophase I of meiosis in mole vole (*Ellobius talpinus* Pallas) with isomorphic (XX) chromosomes in males and females. *Comparative Cytogenetics* 4: 55–66. <https://doi.org/10.3897/comp-cytogen.v4i1.25>
- Král B, Radjabli SI (1974) Banding patterns and Robertsonian fusions in the western Siberian population of *Sorex araneus* (Insectivora, Soricidae). *Folia Zoologica* 23: 217–227.
- La Salle S, Sun F, Zhang XD, Matunis MJ, Handel MA (2008) Developmental control of sumoylation pathway proteins in mouse male germ cells. *Developmental Biology* 321: 227–237. <https://doi.org/10.1016/j.ydbio.2008.06.020>
- Lanzone C, Rodríguez D, Cuello P, Albanese S, Ojeda A, Chillo V, Martí DA (2011) XY₁Y₂ chromosome system in *Salinomys delicatus* (Rodentia, Cricetidae). *Genetica* 139: 1143–1147. <https://doi.org/10.1007/s10709-011-9616-7>
- Lenhossek M (1898) Untersuchungen über Spermatogenese. *Archiv für mikroskopische Anatomie und Entwicklungsgeschichte* 51: 215–318.
- Li Q, Lau A, Morris TJ, Guo L, Fordyce CB, Stanley EF (2004) A syntaxin 1, Galpha(o), and N-type calcium channel complex at a presynaptic nerve terminal: analysis by quantitative immunocolocalization. *Journal of Neuroscience* 24: 4070–4081. <https://doi.org/10.1523/JNEUROSCI.0346-04.2004>
- Lifschytz E, Lindsley D (1972) The role of X-chromosome inactivation during spermatogenesis. *Proceedings of the National Academy of Sciences of the United States of America* 69: 182–186. <https://doi.org/10.1073/pnas.69.1.182>
- Mahadevaiah SK, Bourc'his D, de Rooij DG, Bestor TH, Turner JM, Burgoyne PS (2008) Extensive meiotic asynapsis in mice antagonises meiotic silencing of unsynapsed chromatin and consequently disrupts meiotic sex chromosome inactivation. *Journal of Cell Biology* 182: 263–276. <https://doi.org/10.1083/jcb.200710195>
- Mahadevaiah SK, Turner JMA, Baudat F, Rogakou EP, de Boer P, Blanco-Rodriguez J, Jasin M, Keeney S, Bonner WM, Burgoyne PS (2001) Recombinational DNA double-strand breaks in mice precede synapsis. *Nature Genetics* 27: 271–276. <https://doi.org/10.1038/85830>
- Matveevsky S, Bakloushinskaya I, Kolomiets O (2016) Unique sex chromosome systems in *Ellobius*: How do male XX chromosomes recombine and undergo pachytene chromatin inactivation? *Scientific Reports* 6: 29949. <https://doi.org/10.1038/srep29949>
- Matveevsky SN, Pavlova SV, Acaeva MM, Kolomiets OL (2012) Synaptonemal complex analysis of interracial hybrids between the Moscow and Neroosa chromosomal races of the common shrew *Sorex araneus* showing regular formation of a complex meiotic configuration (ring-of-four). *Comparative Cytogenetics* 6: 301–314. <https://doi.org/10.3897/CompCytogen.v6i3.3701>
- McKee BD, Handel MA (1993) Sex chromosomes, recombination, and chromatin conformation. *Chromosoma* 102: 71–80. <https://doi.org/10.1007/BF00356023>
- Mercer SJ, Wallace BMN, Searle JB (1992) Male common shrews (*Sorex araneus*) with long meiotic chain configurations can be fertile: implications for chromosomal models of speciation. *Cytogenetics and Cell Genetics* 60: 68–73. <https://doi.org/10.1159/000133298>

- Metzler-Guillemain C, Depetris D, Luciani JJ, Mignon-Ravix C, Mitchell MJ, Mattei M-G (2008) In human pachytene spermatocytes, SUMO protein is restricted to the constitutive heterochromatin. *Chromosome Research* 16: 761–782. <https://doi.org/10.1007/s10577-008-1225-7>
- Moens PB, Tarsounas M, Morita T, Habu T, Rottinghaus ST, Freire R, Jackson SP, Barlow C, Wynshaw-Boris A (1999) The association of ATR protein with mouse meiotic chromosome cores. *Chromosoma* 108: 95–102. <https://doi.org/10.1007/s004120050356>
- Namekawa SH, Lee JT (2009) XY and ZW: is meiotic sex chromosome inactivation the rule in evolution? *PLoS Genetics* 5: e1000493. <https://doi.org/10.1371/journal.pgen.1000493>
- Narain Y, Fredga K (1997) Meiosis and fertility in common shrew, *Sorex araneus*, from a chromosomal hybrid zone in central Sweden. *Cytogenetics and Cell Genetics* 78: 253–259. <https://doi.org/10.1159/000134668>
- Noronha RR, Nagamachi CY, O'Brien PCM, Ferguson-Smith MA, Pieczarka JC (2009) Neo-XY body: an analysis of XY₁Y₂ meiotic behavior in *Carollia* (Chiroptera, Phyllostomidae) by chromosome painting. *Cytogenetic and Genome Research* 124: 37–43. <https://doi.org/10.1159/000200086>
- Ohno S, Kaplan WD, Kinoshita R (1958) A photomicrographic representation of mitosis and meiosis in the male of *Rattus norvegicus*. *Cytologia* 23: 422–428. <https://doi.org/10.1508/cytologia.23.422>
- Pack SD, Borodin PM, Serov OL, Searle JB (1993) The X-autosome translocation in the common shrew (*Sorex araneus* L.): late replication in female somatic cells and pairing in male meiosis. *Chromosoma* 102: 355–360. <https://doi.org/10.1007/BF00661279>
- Painter TS (1924) Studies in mammalian spermatogenesis. III. The fate of the chromatin-nucleolus in the opossum. *Journal of Experimental Zoology* 39: 197–227. <https://doi.org/10.1002/jez.1400390203>
- Pathak S, Lin CC (1981) Synaptonemal complex of the sex-autosome trivalent in a male Indian muntjac. *Chromosoma* 82: 367–376. <https://doi.org/10.1007/BF00285762>
- Pavlova SV, Kolomiets OL, Bulatova N, Searle JB (2008) Demonstration of a WART in a hybrid zone of the common shrew (*Sorex araneus* Linnaeus, 1758). *Comparative Cytogenetics* 2: 115–120.
- Rasband WS (1997–2016) ImageJ. U.S. National Institutes of Health, Bethesda, MD.
- Ratomponirina C, Viegas-Péquignot E, Dutrillaux B, Petter F, Rumpler Y (1986) Synaptonemal complexes in Gerbillidae: probable role of intercalated heterochromatin in gonosome–autosome translocations. *Cytogenetics and Cell Genetics* 43: 161–167. <https://doi.org/10.1159/000132315>
- Reitan NK, Sporsheim B, Bjørkøy A, Strand S, Davies C de L (2012) Quantitative 3-D colocalization analysis as a tool to study the intracellular trafficking and dissociation of pDNA-chitosan polyplexes. *Journal of Biomedical Optics* 17: 026015. <https://doi.org/10.1117/1.JBO.17.2.026015>
- Rogers RS, Inselman A, Handel MA, Matunis MJ (2004) SUMO modified proteins localize to the XY body of pachytene spermatocytes. *Chromosoma* 113: 233–243. <https://doi.org/10.1007/s00412-004-0311-7>
- Sachs L (1955) The possibilities of crossing-over between the sex chromosomes of the house mouse. *Genetica* 27: 309–322. <https://doi.org/10.1007/BF01664166>

- Sciurano RB, Rahn MI, Rossi L, Luaces JP, Merani MS, Solari AJ (2012) Synapsis, recombination, and chromatin remodeling in the XY body of armadillos. *Chromosome Research* 20: 293–302. <https://doi.org/10.1007/s10577-012-9273-4>
- Sciurano RB, Rahn IM, Cavicchia JC, Solari AJ (2013) Dissociation of the X chromosome from the synaptonemal complex in the XY body of the rodent *Galea musteloides*. *Chromosome Research* 20: 293–302. <https://doi.org/10.1007/s10577-013-9379-3>
- Schimenti J (2005) Synapsis or silence. *Nature Genetics* 37: 11–13. <https://doi.org/10.1038/ng0105-11>
- Searle JB, Fedyk S, Fredga K, Hausser J, Volobouev VT (1991) Nomenclature for the chromosomes of the common shrew (*Sorex araneus*). *Mémoires de la Société Vaudoise des Sciences Naturelles* 19: 13–22.
- Searle JB, Wójcik JM (1998) Chromosomal evolution: the case of *Sorex araneus*. In: Wójcik JM, Wolsan M (Eds) *Evolution of Shrews*. Białowieża: Mammal Research Institute, Polish Academy of Sciences, 219–262.
- Sharman GB (1956) Chromosomes of the common shrew. *Nature* 177: 941–942. <https://doi.org/10.1038/177941a0>
- Sharman GB (1991) History of discovery and recognition of XY_1Y_2 systems and chromosome polymorphism in mammals. *Mémoires de la Société Vaudoise des Sciences Naturelles* 19: 7–12.
- Sharp P (1982) Sex chromosome pairing during male meiosis in marsupials. *Chromosoma* 86: 27–47. <https://doi.org/10.1007/BF00330728>
- Solari AJ, Pigozzi MI (1994) Fine structure of the XY body in the XY_1Y_2 trivalent of the bat *Artibeus lituratus*. *Chromosome Research* 2: 53–58. <https://doi.org/10.1007/BF01539454>
- Solari AJ (1974) The behavior of the XY pair in mammals. *International Review of Cytology* 38: 273–317. [https://doi.org/10.1016/S0074-7696\(08\)60928-6](https://doi.org/10.1016/S0074-7696(08)60928-6)
- Turner JM (2007) Meiotic sex chromosome inactivation. *Development* 134: 1823–1831. <https://doi.org/10.1242/dev.000018>
- Turner JMA, Mahadevaiah SK, Benavente R, Offenberger HH, Heyting C, Burgoyne PS (2000) Analysis of male meiotic ‘sex-body’ proteins during XY female meiosis provides new insights into their functions. *Chromosoma* 109: 426–432. <https://doi.org/10.1007/s004120000097>
- Turner JM, Aprelikova O, Xu X, Wang R, Kim S, Chandramouli GV, Barrett JC, Burgoyne PS, Deng CX (2004) BRCA1, histone H2AX phosphorylation, and male meiotic sex chromosome inactivation. *Current Biology* 14: 2135–2142. <https://doi.org/10.1016/j.cub.2004.11.032>
- Turner JM, Mahadevaiah SK, Fernandez-Capetillo O, Nussenzweig A, Xu X, Deng CX, Burgoyne PS (2005) Silencing of unsynapsed meiotic chromosomes in the mouse. *Nature Genetics* 37: 41–47. <https://doi.org/10.1038/ng1484>
- Volobouev V, Granjon L (1996) A finding of the XX/XY_1Y_2 sex-chromosome system in *Taterilus arenarius* (Gerbillinae, Rodentia) and its phylogenetic implications. *Cytogenetics and Cell Genetics* 75: 45–48. <https://doi.org/10.1159/000134455>
- Wahrman J, Richler C, Neufeld E, Friedmann A (1983) The origin of multiple sex chromosomes in the gerbil *Gerbillus gerbillus* (Rodentia: Gerbillinae). *Cytogenetics and Cell Genetics* 35: 161–180. <https://doi.org/10.1159/000131863>

- Wallace BMN, Searle JB (1990) Synaptonemal complex studies of the common shrew (*Sorex araneus*). Comparison of Robertsonian heterozygotes and homozygotes by light microscopy. *Heredity* 65: 359–367. <https://doi.org/10.1038/hdy.1990.105>
- Ye J, Biltueva L, Huang L, Nie W, Wang J, Jing M, Su W, Vorobieva NV, Jiang X, Graphodatsky AS, Yang F (2006) Cross-species chromosome painting unveils cytogenetic signatures for the Eulipotyphla and evidence for the polyphyly of Insectivora. *Chromosome Research* 14: 151–159. <https://doi.org/10.1007/s10577-006-1032-y>
- Yoshida K, Kitano J (2012) The contribution of female meiotic drive to the evolution of the neo-sex chromosomes. *Evolution* 66: 3198–3208. <https://doi.org/10.1111/j.1558-5646.2012.01681.x>